

Multimodal Medical Image Fusion using Guided Filter in NSCT Domain

Nancy Mehta* and Sumit Budhiraja

ECE, UIET, Panjab University, Chandigarh, 160014, India.

*Corresponding author E-mail: nancymehta186@gmail.com

<http://dx.doi.org/10.13005/bpj/1566>

(Received: 16 July 2018; accepted: 19 November 2018)

Multimodal medical image fusion aims at minimizing the redundancy and collecting the relevant information from the input images that are acquired using different medical sensors. The main goal is to produce a single fused image that is more informative and efficient for clinical applications. In this paper modified fusion method has been proposed in which NSCT decomposition is used to decompose the wavelet coefficients obtained after wavelet decomposition. NSCT being multidirectional, shift invariant transform provide better results. Guided filter has been used for the fusion of high frequency coefficients on account of its edge preserving property. Phase congruency is used for the fusion of low frequency coefficients due to its insensitivity to illumination contrast hence making it suitable for medical images. Simulation results show that the proposed technique performs better in terms of entropy, structural similarity index, Piella metric. The fusion response of the proposed technique is also compared with other fusion approaches; proving the effectiveness of the obtained fusion results.

Keywords: Imagefusion, NSCT, Phase congruency, Guided filter, wavelet decomposition.

With advancement in technology, lot of improvement has been seen in the clinical applications and their has been tremendous increase in the number of modality images. Each imaging modality used for medical purposes provides unique information which is not present in any other modality. For proper diagnosis of a disease, doctors require information from more than one modality. CT images provide information regarding the dense structures of bone for proper radiation dose estimation but it does not provide much insight about the soft tissues. MRI images highlight the soft tissue contrast but lack the information about the bones. Hence, due to the incapability of a single image to provide all the information, radiologists require fusion of two or more than two modalities.

Through imagefusion, it is possible to combine information from more than one modalities in a better way by using several techniques¹. CT and MRI image fusion permits concurrent visualization of the soft tissue information given by the MRI image and bony anatomy given by the CT image which helps the doctors in diagnosing the disease and providing better treatment.

Image fusion aims at combining the relevant information from both the images into a single image and while fusing, care should be taken of not introducing any artifacts in the image. Image fusion can be classified into three categories based on merging stage- pixel level, decision level and feature level. Among these pixel level fusion is mostly used in multimodal image fusion

on account of its easy implementation and its capability to retain the original information². In this paper, the focus is on pixel level fusion. Image fusion can be applied in spatial and transform domain. The basic spatial domain methods include averaging, IHS, Brovey method, max-min. But these techniques are not very efficient to fuse the relevant information of the source images and leads to certain artifacts³. The human visual system is able to better preserve the features that exist in different scales. Hence Multiscale Transform domain methods help to solve these shortcomings of spatial domain methods.

In multiscale decomposition methods, the first step is to decompose the image into low and high-frequency subbands at different resolution and then combining the coefficients of different subbands by different fusion rules. Toet *et al.*⁴ introduced various pyramidal techniques for multisensor image fusion. Different pyramidal techniques like gradient pyramid, morphological pyramid, Laplacian pyramid have been used a lot in previous years but they lead to loss of spatial information⁵. The wavelet transform is another transform method for image fusion. In work of Yang *et al.*⁶, wavelet along with maximum energy based selection rule was implemented but it was not able to capture the border line in the fused image. Wavelet decomposition does not give good results while capturing edges and contour in the image⁷. Moreover, it gathers limited directional information in vertical, diagonal and horizontal directions⁸. Dual tree complex wavelet transform⁹ which is an enhancement of DWT was proposed by N.G. Kingsbury but it caused artifacts around the edges.

In order to overcome this shortcoming, number of other multiscale methods have been proposed like shearlet, curvelet, ripplelet, contourlet¹⁰⁻¹³. But the main problem in all these multiscale methods was they lack shift variance which leads to difficulty in capturing the contours and edges in the image. NSCT introduced by Cunha *et al.* is multidirectional, shift invariant and multiscale decomposition transform¹⁴⁻¹⁵. It provides good results in geometric transformations by discarding the sub-sampling operation during decomposition and reconstruction of images and thus can effectively reduce pseudo-Gibbs phenomenon. In

the proposed method, wavelet transform along with NSCT is used for image fusion.

Since fusion rule plays a very important part in deciding the quality of an image, hence different fusion rules have been used for the low and high-frequency coefficients. Phase congruency is the fusion rule selected for the low frequency coefficients and guided filter is used for the high frequency coefficients.

The rest of paper is organized as follows: an overview of NSCT along with phase congruency and guided filter is explained in Section II followed by the proposed multimodal image fusion framework in Section III. Results and discussions are given in Section IV and conclusion is given in part V.

Preliminaries

Non Subsampled Contourlet Transform

NSCT is based on the theory of contourlet transform and consists of two stages including non-sampled directional filter bank (NSDFB) and non-sampled pyramid (NSP). The former performs directional decomposition and the latter performs multidirectional decomposition. Firstly, the image is decomposed into several scales by NSP which results in one low frequency and one high-frequency image at each decomposition level. The number of decompositions at each level can differ making NSCT flexible and valuable for image fusion. The low-frequency component at each NSP level is iteratively decomposed to capture all the singularities. Thus NSP outputs $k+1$ sub-images consisting of one low frequency and k high-frequency images and all the images produced are of the same size as the source image where k represents the number of decomposition levels. Fig.1 shows the NSP decomposition with $k=3$ levels. NSDFB ensures directional decomposition of the high-frequency images obtained from NSP at each level and as a result, produces 2^l directional images at each scale. A four channel NSDFB built from two-channel filter banks is shown in Fig.2d

Non-sampled Pyramid

The non-sampled pyramid consists of two-channel filter bank without any downsamplers which help in removing the frequency aliasing. The frequency response of the filter is shown in Fig. 2b, where $H_k(z)$ ($k=(0,1)$) are the analysis filters and $G_k(z)$, are the synthesis filters and are the building

block of the Nonsubsampled pyramid. Each stage of NSP produces a low-pass filtered image and a bandpass filtered image. For the next level all the filters are upsampled by 2 in both dimensions. NSP has a redundancy of $k+1$ where k is the number of decomposition levels. Figure 1 represents NSP with $k=3$ levels.

Non-subsampled Directional Filter Bank

Bamberger and Smith constructed directional filter bank¹⁶ by combining the resampling operations and critically sampled two-channel filter banks and as a result, a tree-structured filter bank that decomposes the 2d frequency plane into directional wedges is obtained. The L level NSDFB results in 2^L directional subbands which results in directional decomposition of the images. Fig. 2c is showing frequency response of filter bank of NSDFB. It is constructed by iterating this filter bank in order to obtain the directional decomposition. The filters at the next level as shown in Fig. 2d are obtained by upsampling all the filters by a Quincunx matrix that is given by:

$$Q = \begin{pmatrix} 1 & 1 \\ 1 & -1 \end{pmatrix}$$

Frequency divisions obtained with NSCT is shown in Fig. 2e. The number of frequency division depends upon the number of directional images we want at each level.

Phase Congruency

Phase congruency is a contrast invariant feature extraction method based on local energy model which follows the principle that significant features can be found in an image where the Fourier components are maximally in phase with one another. Moreover, it is insensitive to different pixel intensity mapping. It is insensitive to illumination changes and contrast which makes it suitable for use

in multimodal image fusion¹⁷. It provides improved frequency localization which is a good feature for multimodal medical image fusion. Hence it is employed as a fusion rule for the low frequency coefficients in the proposed method.

Guided filter

Guided filter is an edge-preserving linear translation-invariant filter which produces an output image by considering the contents of the input image. It outputs a distortion free result by removing the gradient reversal artifacts. It is a neighborhood operation and consists of an input image t , an output image Q and a guidance image I . The guided filter¹⁸ assumes that the Q is a linear transformation of the guidance image I in a window w_k centered at pixel k and the output image at pixel k can be expressed as

$$Q_i = a_k I_i + b_k \quad \forall i \in w_k \quad \dots(1)$$

$$a_k = \frac{1}{W} \frac{\sum_{i \in w_k} I_i t_i - u_k E[t_k]}{\sigma_k^2 + \epsilon} \quad \dots(1a)$$

$$b_k = E(t_k) - a_k u_k \quad \dots(1b)$$

where a_k and b_k are the coefficients that are constant in w_k . The coefficients a_k and b_k can be found using equations 1a and 1b. $E(t_k)$ represents the mean of input image in window w_k . The mean and variance of the image in window w_k is represented by u_k and σ_k^2 . Guided filter has been used a lot for image fusion and provides good results for multimodal medical image fusion¹⁹. In the proposed technique guided filter by modifying weight maps has been used for the fusion of high frequency NSCT coefficients which preserves the edges and helps in information preservation.

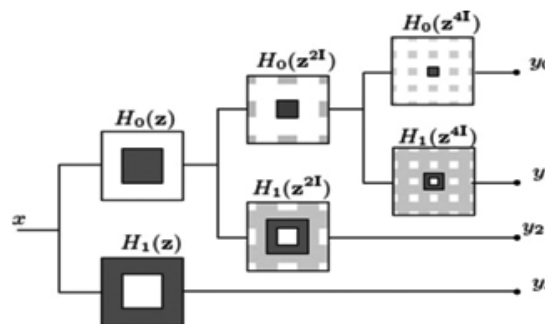


Fig.1. Three stage Non subsampled pyramid decomposition

Proposed Fusion Framework

Fusion is performed on registered source images A and B using wavelet transform and NSCT shown in Fig.3 and Fig.4. Firstly wavelet decomposition is used to decompose the registered source images then NSCT decomposition is performed on the wavelet

reconstructed coefficients. For the low frequency coefficients, phase congruency and for the high frequency coefficients are The complete method is shown in several steps. Step 1 is divided into two stages in which the first stage discusses wavelet decomposition and the second stage discusses about NSCT decomposition. Step 2 explains about

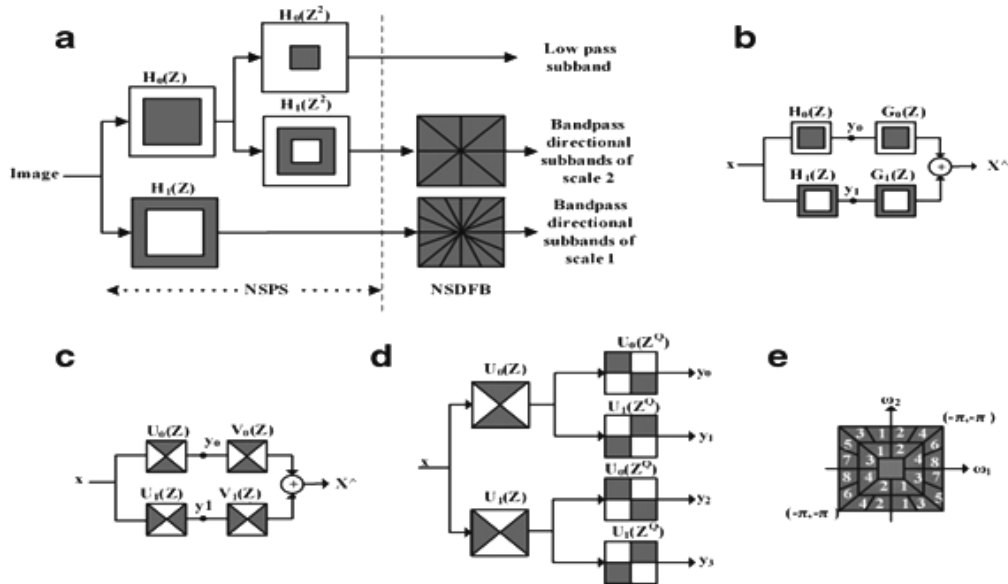


Fig. 2. Non-subsampled contourlet transform a) NSFB structure that implements NSCT b) Two channel NSP filter bank c) Two channel NSDFB d) Four channel NSDFB e) Frequency partitioning with NSCT[14]

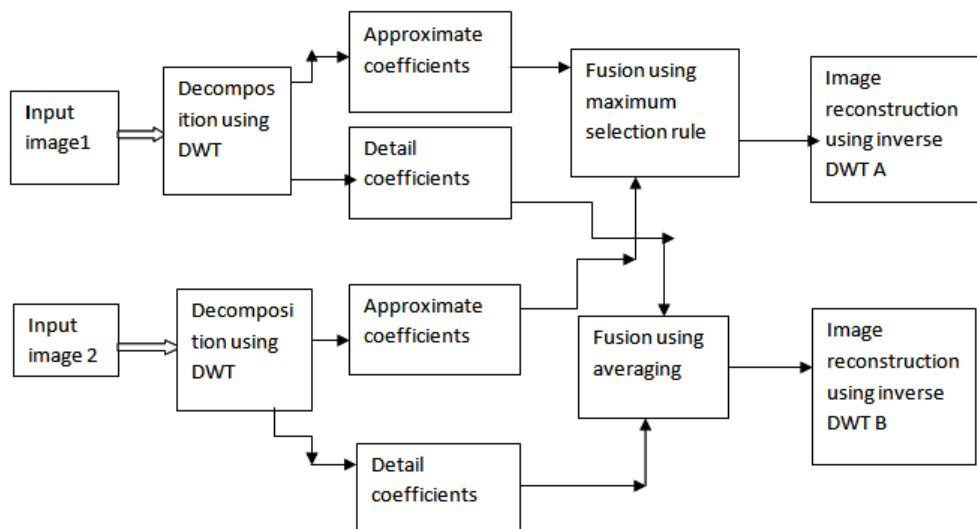


Fig. 3. Block diagram of the wavelet decomposition and reconstruction (Stage 1)

the fusion rule used for low frequency coefficients and in step 3 the fusion rule for high frequency coefficients is used.

Step1. *Stage 1* - Firstly the registered source images are passed through wavelet transform and the approximate and detail coefficients obtained after wavelet decomposition are fused through averaging and maximum selection rule respectively as shown in Fig.3 to obtain two fused images. Haar wavelet on account of its fast implementation has been used for wavelet decomposition and reconstruction.

Step2. *Stage 2*. After NSCT is performed on the wavelet reconstructed images A and B which are decomposed into one low frequency and

series of high-frequency images at each level and direction θ , i.e., $A: \{C_1^A, C_{L,\theta}^A\}$, $B: \{C_1^B, C_{L,\theta}^B\}$. Here C_1 represents the low-frequency images and $C_{L,\theta}$ are the high frequency images at level L and orientation θ . The number of decomposition levels in the method is [2 1 0] which represents 4 directional images in the first level, 2 directional images in the second level and 1 directional image in the third level. A table comparing the different decomposition levels with different directional sub images has been shown in the Table 1.

Step2. *Fusion of low-frequency coefficients*: The low frequency sub-image coefficients represent the average information of the image and determine the outline of images. In order to construct the

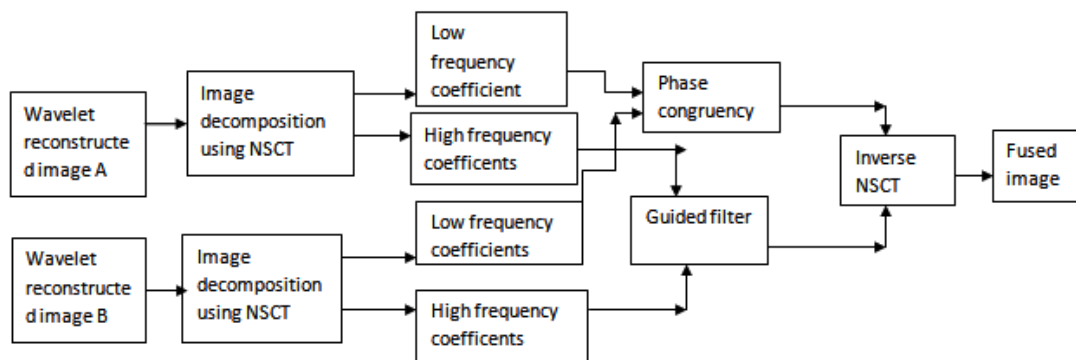


Fig. 4. Block diagram of NSCT decomposition and reconstruction (Stage 2)



Fig. 5. Different sets of CT and MRI images

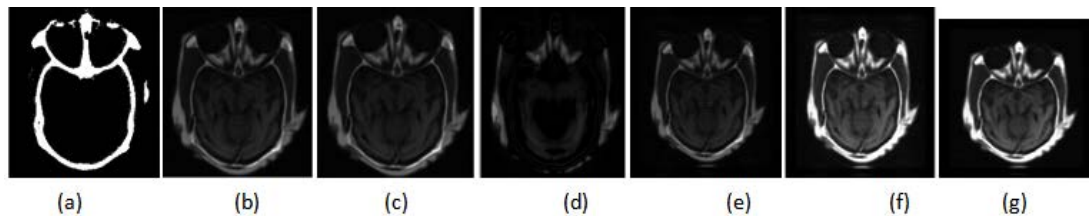


Fig. 6. Multimodal medical image fusion results of image dataset 1 using different techniques (a) PCA based fusion (b) Wavelet with 3 levels (c) Wavelet with 1 level (d) Guided filter (e) NSCT1 (f) NSCT2 (g) Proposed technique

approximate information mostly averaging method is used but it results in reduced contrast in the image and thus reducing the quality of the image. In this method phase congruency is used as a fusion rule in which the features are first extracted using from P_{CI}^A

and P_{CI}^B and then fusion is done according to

$$P = \frac{\sum W^{s,x,y} [A^{s,x,y}] (\cos(\theta^{s,x,y}))}{\sum_n A_{x,y} + \epsilon} \dots(2)$$

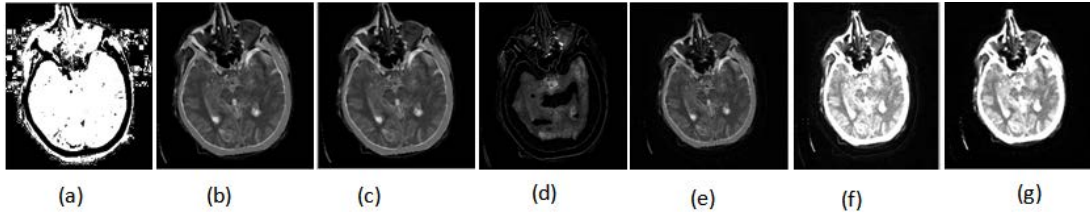


Fig.7. Multimodal medical image fusion results of image dataset 2 using different techniques (a)PCA based fusion (b) Wavelet with 3 levels (c)Wavelet with 1 level (d) Guided filter (e)NSCT1 (f)NSCT2 (g)Proposed technique

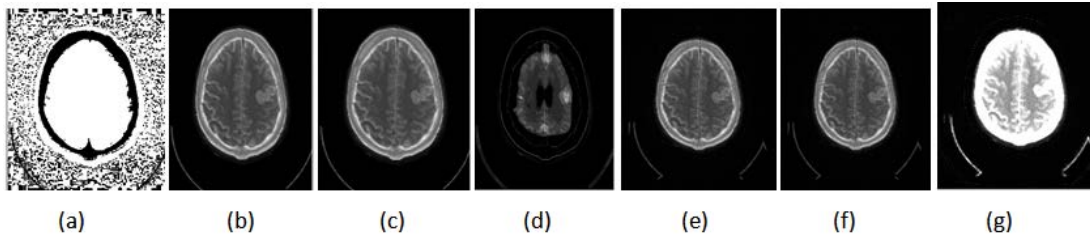


Fig. 8. Multimodal medical image fusion results of image database 3 using different techniques : (a)PCA based fusion, (b)wavelet with 3 levels (c)wavelet with 1 level (d) Guided filter with $r=3, E=0.005$ (e) NSCT1 (f) NSCT2 (g) proposed NSCT method

$$C_1^F(x,y) = C_1^A(x,y), \text{ if } P_{CI}^A(x,y) > P_{CI}^B(x,y) \dots(3)$$

$$C_1^F(x,y) = C_1^B(x,y), \text{ if } P_{CI}^B(x,y) > P_{CI}^A(x,y) \dots(4)$$

$$C_1^F(x,y) = (C_1^B(x,y) + C_1^A(x,y)) / 2, \text{ if } P_{CI}^A(x,y) = P_{CI}^B(x,y) \dots(5)$$

Step3. Fusion of high frequency coefficients: The detail component of source images is contained in the high frequency images. Basically they contain information related to detail and features of an image like texture. Noise also has a relation with high frequencies and may lead to introduction of certain artifacts hence we need to choose a fusion rule which is better for dealing with noisy images²¹. In this paper guided filter has been used to fuse the high frequency components.

$$Q_i = \frac{1}{|w|} \sum_{i \in w} (a_k I_i + b_k)$$

In this approach, guidance image is the high-frequency coefficient of image $AC_{L,A}$ and input

Fig. 9. Performance of the proposed technique by varying the window radius

Window radius	entropy	QP	SSIM	MI
0.01	6.4274	0.9892	0.9967	0.6192
0.1	5.965	0.9776	0.9865	0.546
1	5.2514	0.9629	0.9667	0.432
10	2.8315	0.6181	0.651	0.345

image is the high frequency coefficient of image B C_L^B to produce an output image at each level. Then all the high frequency images are fused together by simple averaging to produce $C_{1_i}^F$. Step4. Inverse NSCT is performed on the $C_{1_i}^F$ and $C_{1_i}^F$ to get the fused image F.

RESULTS AND DISCUSSIONS

To fulfill the requirements of fusion algorithm of being robust, simple and effective the results has been evaluated subjectively as well as objectively. The subjective evaluation is based on human visual characteristics and knowledge of the observer and the objective evaluation is done according to certain statistical parameters.

Performance parameters for evaluation of image fusion

1) Normalized Mutual Information²² Q_{MI} : It is a quantitative measurement of the dependence of the fused image on the input source images. It is desirable to have large values of MI.

$$QMI = 2 \frac{(MI(A,F) + MI(B,F))}{(H(A)+H(F)) + (H(B)+H(F))} \dots(6)$$

Table 1. Simulation results for proposed technique using different decomposition levels

Decomposition level	Entropy for dataset 1	Piella metric for dataset 1	Time in seconds
[2 1]	6.2860	0.9872	59
[2 1 0]	6.4686	0.9893	64
[2 1 1]	6.40	0.9889	70
[3 2 1]	6.4297	0.9878	178
[2 2 1 1]	5.7848	0.9862	117
[4 2]	5.621	0.9859	474
[4 2 2]	5.609	0.9850	507

Table 2. Simulation results for proposed technique using different data sets

Image dataset	Entropy	Q_p	SSIM	MI
1	6.4686	0.9893	0.9967	0.6192
2	5.5322	0.9865	0.997	0.567
3	5.1273	0.9854	0.9972	0.589

$$MI(A,F) = H(A) + H(F) - H(A,F) \dots(7)$$

where $H(A), H(B), H(F)$ are the marginal entropies of image A, image B, and image F respectively. $MI(A,F)$ represent the mutual information between image A and image F. $H(A,F)$ represents the joint entropy between image A and F.

2) Structural Similarity Index (SSIM) Q_Y : It signifies the capability of the fused technique to capture the structural information in an image.

$$QY = S_w SSIM(A_w, F_w) + (1 - S_w) SSIM(B_w, F_w) \dots(8)$$

$$= \max \{ SSIM(A_w, F_w), SSIM(B_w, F_w) \}$$

if $SSIM(A_w, B_w) \geq 0.75$

$$= \min \{ SSIM(A_w, F_w), SSIM(B_w, F_w) \}$$

if $SSIM(A_w, B_w) \leq 0.75$

... (9)

$$S_w = \frac{s(A_w)}{s(A_w) + s(B_w)} \dots(10)$$

Here $s(A_w)$ and $s(B_w)$ are the variances of the source input images A and B of size [7 7] and w is a sliding window which moves through all the pixels and S_w is the local weight that is obtained from local image variance. The detailed implementation of the above technique is given in²³.

3.) Entropy: It predicts the amount of information content in an image.

$$E(u) = -\sum p(u) \log_2 p(u) \dots(11)$$

Here $p(u)$ gives the marginal probability distribution.

4.) Piella and Heijman's metric (Q_p)²⁴: It provides the structural and edge information in an image.

$$\xi_{P1} = \frac{1}{w} \sum_{w \in W} [S_w Q_0(A, F|w) + (1 - S_w) Q_0(B, F|w)] \dots(12)$$

Here $Q_0(A, F|w)$ and $Q_0(B, F|w)$ are the local quality indexes calculated in a sliding window w and S_w is

Table 3. Evaluation Indices for Medical Images of dataset 1 using different techniques

Technique	Entropy	Q_p	SSIM	Q_{MI}
Wavelet level 1	6.05	0.5605	0.665	0.5294
Wavelet level 3	6.039	0.6607	0.685	0.6384
NSCT2	6.105	0.9970	0.9958	0.580
Guided filter	4.368	0.4276	0.8070	0.670
PCA	3.67	0.3031	0.458	0.781
NSCT1	5.73	0.745	0.876	0.591
Proposed method	6.4686	0.9893	0.9967	0.6192

defined as:

$$S_w = \frac{\sigma_A}{\sigma_A + \sigma_B} \quad \dots(13)$$

Here σ_A and σ_B represents the variance of source images A and B.

5.)Cvejic’s metric(Q_C)²⁵: It indicates how by minimizing the distortion information is preserved in the output image. It is calculated as:

$$Q_C = \mu(A_w, B_w, F_w) UIQI(A_w, F_w) + (1 - \mu(A_w, B_w, F_w)) UIQI(B_w, F_w) \quad \dots(14)$$

Where μ is calculated as:

$$\mu(A_w, B_w, F_w) = 0 \quad \text{if} \quad \frac{\sigma_{AF}}{\sigma_{AF} + \sigma_{BF}} < 0 \quad \dots(15)$$

$$= \frac{\sigma_{AF}}{\sigma_{AF} + \sigma_{BF}} \quad \text{if} \quad 0 \leq \frac{\sigma_{AF}}{\sigma_{AF} + \sigma_{BF}} < 1 \quad \dots(16)$$

$$= 1 \quad \text{if} \quad \frac{\sigma_{AF}}{\sigma_{AF} + \sigma_{BF}} > 1 \quad \dots(17)$$

Here μ represents the covariance between image A and F and σ_{BF} represents the covariance between images B and F. UIQI is the universal image quality index²⁶.

Simulation results on CT and MRI images

The registered images of size 256*256 are taken from med.harvard.edu/aanlib/home.html. To evaluate the performance of the proposed technique an image database consisting of CT and MRI images shown in Fig. 5 is used. The corresponding pixels of the source images have been registered. The images are of size 256*256 with 256-level grayscale. The results of the proposed fusion framework are compared with traditional PCA, Wavelet with 1 level decomposition, Wavelet with 3 level decomposition, NSCT2 in which averaging for low-frequency coefficients and maximum selection rule for high-frequency coefficients has been used, NSCT1 in which phase congruency for low and guided filter for high frequency components is used but without wavelet decomposition. The level of decomposition for NSCT is 3. The reason for using 3 level of decomposition is shown in table 1. For wavelet-based method averaging is used for the approximate coefficients and maximum fusion rule is used for high-frequency coefficients. For implementing NSCT maximally flat filters is used for pyramid decomposition and diamond maxflat filters are used for directional decomposition. The guided filter implemented in the technique has

modified by using different levels for the weight maps. Window radius and epsilon value for the guided filter is set to $r=0.01$ and [18]. Comparison of the objective parameters for different values of epsilon and radius has been shown in Fig9. The wavelet decomposition method used in the implemented technique has levels=3. Haar wavelet has been used for wavelet decomposition.

From the figure 6 it is clear that the proposed technique is able to preserve the details as well as lead to better quality image. Figure 7 represents the fused image of CT and MRI showing multiple embolic infarctions and the proposed technique is able to retain most of the information. Figure 8 represents the fused CT and MRI image showing acute stroke of speech arrest.

Table 1 shows the values of entropy and Piella metric for different decomposition levels. From the table it is clear that less number of levels takes less computation time. Increasing the number of directional decompositions at each scale also lead to higher computation time and the image quality is also affected by increasing the number of levels. Level [2 1] takes the least time but the value of Q_p metric is less. The decomposition level [2 10] provides better results for entropy, computation time and Piella metric. Hence in the proposed methodology the decomposition level is [2 1 0].

Table 2 represents the values of different metrics for datasets 1, 2 and 3 using the proposed technique. Entropy represents the information content and its value should be high. Q_p value should be close to 1 which represents the edge information and SSIM should also be close to 1 to represent the structural similarity.

From the Fig.9 it is clear that increasing the value of window radius leads to reduced value of entropy, SSIM, Q_p as it leads to loss of edge information. Hence the value for window radius is set to 0.01.

The comparison of statistical parameters for the fused image by using different techniques for the image dataset 1 has been shown in Table2. It is clear that the implemented technique performs better by preserving the spectral and spatial information. PCA based results are not so good as compared to other techniques as it does not provide information at different scales. Guided filter technique is better in preserving the edges but it leads to reduced spatial information. Wavelet

techniques are not able to preserve information at the edges hence the value of statistical parameters decreases for them. NSCT 1 method in which wavelet decomposition is not done prior to NSCT has low value of entropy and Q_p , hence proving the need of using wavelet before NSCT. NSCT2 also has low value of the objective parameters.

Proposed NSCT performs better in terms of entropy, SSIM, Q_p and thus showing the effectiveness of the method on account of its capability to capture the point regularities in an image. Though the value of mutual information is not as good.

CONCLUSION

In this paper, modified fusion framework for multimodal medical images based on nonsubsampled contourlet transform and guided filter has been proposed. Wavelet decomposition is done prior to NSCT for visually better results. For low-frequency bands of NSCT phase congruency and for high-frequency bands guided filter is used. Further, in order to prove the practical applicability of the proposed method, two sets of images of human brain affected with cerebrovascular diseases of acute stroke with speech arrest and multiple embolic infarctions is taken. The visual analysis reveals that the proposed method is able to preserve the soft tissue details of MRI and bony structure of CT image. Though mutual information is not so good but it can be improved by further modifications. Further, the proposed method can be applied to fuse the functional medical images and anatomical medical images that are represented by color and grayscale images respectively. The guided filter used for high frequency coefficients fusion can be made adaptive for further improvement in results.

REFERENCES

- Amdur RJ, Gladstone D, Leopold KA, Harris RD. Prostate seed implant quality assessment using MR and CT image fusion. *Int J Radiat Oncol Biol Phys.*; **43**:67–72 (1999). doi: 10.1016/S0360-3016(98)00372-1.
- R. Redondo, F. Sroubek, S. Fischer, and G. Cristobal, "Multifocus image fusion using the log-Gabor transform and a multisize window technique," *Inf. Fusion*, **10**(2): pp. 163–171 (2009).
- A. P. James and B. V. Dasarathy, "Medical image fusion: A survey of the state of the art," *Inf Fusion* . **19**, pp. 4-19: (2014).
- Toet A, van Ruyven LJ, Valetton JM. Merging thermal and visual images by a contrast pyramid. *Opt Eng.*; **28**: 789–792 (1989). doi: 10.1117/12.7977034.
- V.S. Petrovic and C. S. Xydeas, "Gradient-based multiresolution image fusion," *IEEE Trans., Image Processing*, **13**(2): pp. 228-237: (2004).
- Y. Yang, D. S. Park, S. Huang, and N. Rao, "Medical image fusion via an effective wavelet-based approach," *EURASIP Journal Advanced Signal Processing*, **20**(10): pp. 1–13 (2010).
- Z. Liu, H. Yin, Y. Chai, and S. X. Yang, "A novel approach for multimodal medical image fusion," *Expert Systems with Applications*, **41**: pp. 7425–7435 (2014).
- F. E. Ali, I. M. El-Dokany, A. A. Saad, and F. E. Abd El-Samie, "Curvelet fusion of MR and CT images," *Progr. Electromagn. Res. C*, **3**: pp. 215–224 (2008).
- Selesnick IW, Baraniuk RG, Kingsbury NG. The dual-tree complex wavelet transform. *IEEE Signal Process Mag.*; **22**:123–151 (2005). doi: 10.1109/MSP.2005.1550194.
- S. Serikawa, H. Lu, Y. Li and L. Zhang, "Multimodal medical image fusion in modified Sharp frequency localized contourlet domain", in *Proc. IEEE Computer Society 13th ASIC Int. Conf. Software Engg., Artificial Intelligence, Networking, and Parallel/ Distributed Computing*, pp. 33-37 (2012).
- M.J. Choi, R.Y. Kim, and M.G. Kim, "The curvelet transform for image fusion," *ISPRS*, **35**: pp 59-6 (2004).
- X. Zhou, W. Wang, and R. Liu, "Compressive sensing image fusion algorithm based on directionlets," *EURASIP J. Wireless Communication and Networking*, Feb. (2014)
- L. Wang, B. Li, and L. Tian, "EGGDD: AN explicit dependency model for multimodal-medical image fusion in the shift-invariant shearlet transform domain," *Information Fusion*, **19**: pp. 29-37 (2014).
- G. Bhatnagar, Q. M. J. Wu, and Z. Liu, "Directive contrast based multimodal medical image fusion in NSCT domain," *IEEE Trans. Multimedia*, **15**(5): pp. 1014-1024, (2013).
- A. L. da Cunha, J. Zhou, and M. N. Do, "The nonsubsampled contourlet transform: Theory, design, and applications," *IEEE Trans. Image Process.*, **15**(10): pp. 3089–3101 (2006).
- R. H. Bamberger and M. J. T. Smith, "A filter

- bank for the directional decomposition of images: Theory and design," *IEEE Trans. Signal Process.*, **40**(4), pp. 882–893 (1992).
17. Kovsesi, P., Image features from phase congruency. *Video: A Journal of Computer Vision Research*, **1**(3), pp. 2-26 (1999).
 18. S. Li, X. Kang, and J. Hu, "Image fusion with guided filtering," *IEEE Transactions on Image Processing*, **22**(7): (2013).
 19. A. Jameel, A. Ghafoor, and M.M. Riaz, "Improved guided image fusion for magnetic resonance and computed tomography imaging," *Hindawi The Scientific World Journal*, (2014).
 20. N. Wang, Y. Ma, K. Zhan, and M. Yuan, "Multimodal medical image fusion framework based on simplified PCNN in nonsubsamped contourlet transform domain," *Multimedia*, **8**(3): pp. 270–276 (2013).
 21. C. He, Y. Qin, G. Cao and F. Lang, "Medical image fusion using guided filtering and pixel screening based weight averaging scheme," *Academics J. Inc. Journal of Software Engineering*, **7**(2): pp. 77- 85 (2013).
 22. M. Hossny, S. Nahavandi, and D. Creighton, "Comments on information measure for the performance of image fusion," *Electronics Letters*, **36**(4): pp. 308-309 (2000).
 23. C. Yang, J. Zhang, X. Wang, and X. Liu, "A novel similarity based quality metric for image fusion," *Inf. Fusion* **9**: pp. 156–160 (2008).
 24. G. Piella and H. Heijmans, "A new quality metric for image fusion," in *Proceedings of the International Conference on Image Processing (ICIP'03)*, pp. 173-176: (2003).
 25. N. Cvejic, A. Loza, D. Bull, and N. canagarajah, "A similarity metric for assessment of image fusion algorithms." *Inf. Fusion*, **9**(2): pp- 156-160: (2008).
 26. Z. Wang and A. Bovik, "A universal image quality index," *IEEE Signal Process. Letters*, **9**(3): pp. 81–84: (2002).